



*Dedicated to the memory of
Professor Ioan Silaghi-Dumitrescu (1950 – 2009)*

NITRITE LINKAGE ISOMERISM IN HEMES AND RELATED COMPLEXES - MODULATION BY METAL, OXIDATION STATE, MACROCYCLE, AND MEDIUM POLARITY

Radu SILAGHI-DUMITRESCU,^{a*} Matei-Maria UTA^a and Sergei V. MAKAROV^b

^a"Babes-Bolyai" University, Department of Chemistry and Chemical Engineering, 11 Arany Janos str, Cluj-Napoca RO-400028, Roumania

^bState University of Chemistry and Technology, Engels str., 7, 153000 Ivanovo, Russia, E-mail: makarov@isuct.ru

Received March 30, 2010

The nitro/nitrito linkage isomerism in metal-nitrite complexes has been shown to be at work in heme proteins and related inorganic catalytic systems such as phthalocyanines. Here, a systematic examination of the nitro/nitrito isomerism is undertaken with computational methods aiming to identify factors controlling it. The systems addressed include iron and cobalt in formal oxidation states of +1, +2 and +3 and complexed by porphyrin, porphyrazine and phthalocyanine. The oxygen-bound isomer (nitrito) is found to be favored by lower-valence states and by porphyrazine; porphyrin favors the nitrogen-bound isomer (nitro), but these preferences can be modulated by the axial ligand. The dielectric constant of the medium is computed to have minimal effects, of at most 1 kcal/mol; the sign of this effect appears to change depending on the density functional and on the solvation model used.

INTRODUCTION

The nitro/nitrito linkage isomerism is a well-established part of transition metal inorganic chemistry, and entails binding of nitrite to a metal either via a nitrogen atom (nitro isomer, also designated N- in the present work) or via an oxygen atom (nitrito isomer, also designated O- in the present work). Until recently, the role of nitrite linkage isomerism in catalysis has been ignored or considered negligible.¹ We have however shown that product distribution and kinetics of nitrite reduction by phthalocyaninates and porphyrazines of iron or cobalt are best interpreted if one assumes that nitrite binding to these complexes in the catalytic cycle is subjected to linkage isomerism and that this isomerism is controlled by metal identity, oxidation state, and

by macrocycle.^{2,3} We have also predicted, using density functional calculations (DFT) that nitrite linkage isomerism should be at work in metalloproteins such as the heme-containing nitrite reductases¹ or copper-containing nitrite reductases;⁴ this was at odds with previously-known structural experimental data, according to which nitrite would bind to heme proteins only via the nitrogen, and to copper only via the oxygen.^{1,4} More recently, our predictions were confirmed by experimental data, as Richter-Addo and co-workers have shown crystal structures of hemoglobin and myoglobin with nitrite bound to the iron via the oxygen atom; notably, both of these proteins exhibit some nitrite reductase activity thought to be medically-relevant.⁵⁻⁸ Here, our previous computational data are extended in the first systematic attempt to identify factors controlling nitrite linkage isomerism.

* Corresponding author: rsilaghi@chem.ubbcluj.ro

RESULTS AND DISCUSSION

Figure 1 shows the structures of the macrocycles examined here. Formal oxidation states of +1, +2 and +3 were assumed for each metal, and the charge of the system adjusted accordingly, taking into account that the

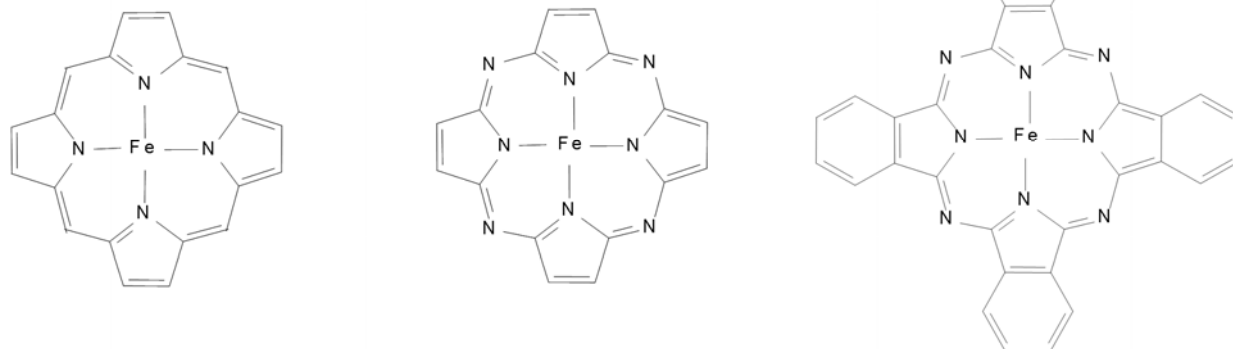


Fig. 1 – Structures of the macrocycles examined here (from left to right: porphyrin, porphyrazine, phthalocyanine). The metal was iron as indicated, or, in its place, cobalt.

Table 1 illustrates the performance of two functionals with two different basis sets and various solvation procedures on the energy difference between the nitro and nitrito isomers of the nitrite adduct of Fe(II) porphyrinate. The largest difference brought about by changes in functional and basis set is ~ 3.5 kcal/mol; given caveats noted by us on related systems for the B3LYP/lanl2dz approach,⁹ the ~ 2.5 kcal/mol difference between the B3LYP and BP86 functionals is probably better illustrative of the intrinsic error margins brought about by functional and basis sets. The magnitude of solvent effects, regardless of functional, solvation model or medium dielectric constant, seems to be restricted to at most ~ 1 kcal/mol; however, the sign of this effect does seem to be influenced by the computational approach.

Table 2 lists energetical preferences for the nitro compared to nitrito isomers of the iron and cobalt macrocycles. Many of the energy differences are larger than the methodology errors suggested by Table 1. The nitro isomer seems to be the more stable one in all cases. The nitrito isomer is most favored by lower metal oxidation states, with the iron (I) porphyrinate appearing most efficient in this respect. Among the complexes featuring metals in the +1 formal oxidation state, the energy differences between the nitro and nitrito isomers show very little dependence on metal. For

macrocyclic ligand contributes with a charge of -2 due to its deprotonated nitrogen atoms, and the nitrite ligand contributed with a charge of -1; $S=0$ and $S=1/2$ spin states were assumed. Axial ligation was provided by nitrite as nitrite or nitro isomer, as indicated in tables.

the complexes featuring metals in the +2 oxidation state, the nitro isomer is more favored with iron compared to cobalt, whereas the reverse trend is seen for the +3 oxidation state. Among the three macrocycles, porphyrazine appears most adept at favoring the nitrito isomer.

Tables 3 and 4 illustrate geometrical and electronic structure features of the Table 2 complexes, and Figure 2 shows some representative optimized geometries. As expected, the equilibrium geometry of the nitro ligand appears insensitive to metal oxidation identity, state and macrocycle, with changes of at most 0.02 Å in N-O bond lengths across various models and with similar variability in Fe-N/O distances; within these limits, higher metal oxidation states lead to shorter N-O bond lengths.

The Fe-NO₂ bond length in the nitro isomer is slightly (0.01-0.02 Å) affected by the nature of the macrocycle, with the general trend $P \leq Pc \leq Pz$; this trend is conserved when it comes to the Fe-O(nitrito) bond length within the nitrito isomer and shows a good inverse correlation with the size of the metal-chelating cavity of the macrocycle as expressed by bond lengths between metal and the four macrocycle nitrogen ligands, which follow the trend $Pz \leq Pc \leq P$. One reason for the latter variation (in iron-macrocycle bond lengths) is that, upon going from porphyrin to porphyrazine four carbon atoms are replaced with nitrogen within the

chelating ring. On the other hand the smaller difference between the porphyrazines and phthalocyanines is mainly due to purely geometrical as opposed to electronic structure reasons: one carbon bond of each pyrrolic ring becomes fused with a phenyl moiety in phthalocyanine; participation in a phenyl ring takes this particular carbon-carbon bond from the 1.37-

1.38 Å invariably seen in porphyrazines and porphyrins to 1.41-1.42 Å in all phthalocyanines examined here, which in turn implies a widening of the pyrrolic rings in Pc, which may also be quantified by an average increase of the N-C-N angle within the pyrrole rings by 2°.

Table 1

Effect of functional, basis set and solvation model on the energy difference (in kcal/mol) between the nitro and nitrito isomers of Fe(II) porphyrinate. The difference obtained with UBP86/6-31G** is taken as reference (see Table 2 for the actual value of this reference)

model	$\Delta\Delta E^-$	model	$\Delta\Delta E^-$	model	$\Delta\Delta E^-$
BP86/6-31G**	0	B3LYP/6-31G**	-2.6	+ CPCM, $\epsilon=80$	-2.5
+ PCM, $\epsilon=4.3$	0.8	+ PCM, $\epsilon=4.3$	-2.2	BP86/lanl2dz	-1.5
+ CPCM, $\epsilon=4.3$	0.5	+ PCM, $\epsilon=80$	-1.5	B3LYP/lanl2dz	-3.5
+ CPCM, $\epsilon=80$	1	+ CPCM, $\epsilon=4.3$	-2.7		

Table 2

Relative energies (N- minus O-, kcal/mol) for pentacoordinated models with Fe and Co. P=porphyrin, Pz=porphyrazine, Pc=phthalocyanine

Model	P	Pz	Pc	Model	P	Pz	Pc
S=1/2 Fe(I)	3.1	2.0	4.3	S=0 Co(I)	3.3	2.3	3.1
S=0 Fe(II)	10.7	9.4	9.8	S=1/2 Co(II)	3.3	2.4	-
S=1/2 Fe(III)	6.9	7.0	8.9	S=0 Co(III)	9.8	9.5	9.9

As a general rule, in most complexes the metal was displaced out of the macrocycle plan towards the axial nitro/nitrito ligand, which resulted in a doming-type distortion¹⁰ of the macrocycle. However, in cases where the metal-axial ligand bond was strongest, a saddling-type distortion¹⁰ was noted; representative examples of domed and saddled geometries for the nitro and nitrito isomers are illustrated in Figure 2.

An expected asymmetry in N-O bond lengths is noted within each nitrito complex, with the MO-NO (M=metal) bond distinctly weakened by coordination to the metal. Increases in formal charge at the metal lead to shorter M-O bond lengths and, as a consequence, longer MO-NO bonds and shorter MON-O bonds. Thus, the MON-O bond lengths vary from 1.25 Å in Fe(I)-nitrito complexes (essentially identical to nitro complexes and suggesting very little activating effect of the

low-valent metal), to 1.21 Å in Fe(III)-nitrito complexes. Meanwhile, the MO-NO bond lengths vary from 1.31 Å in the low-valent complexes to 1.34 Å in ferric nitrito complexes.

The order of metal-N(nitro) bond lengths is $Co \geq Fe$. Somewhat counterintuitive is the shorter metal-N(nitro) bond length seen in the M(I) nitro adducts compared to their M(II) counterparts: the higher electron density at a metal(I) center would have been expected to lengthen, not shorten, metal-ligand bonds. However, as shown below, the formally metal(I) systems appear to instead harbor at least one reducing equivalent on the macrocycle with the metal better described as M(II).

The nitrite ligand tends to carry less electron density (on average by 0.1 units) in the nitrito than in the nitro isomer; this difference may be traced to the nitrogen atom, which carries distinctly more positive charge in the nitro isomer compared to the

nitrito, thus reflecting direct ligation (or lack thereof) of the nitrogen to the metal; by contrast, the partial atomic charges on the oxygen are essentially unaffected by the linkage mode. This

difference in charge behavior between oxygen and nitrogen is in line with the nitrogen being a softer center and hence more adept at delocalizing charge.

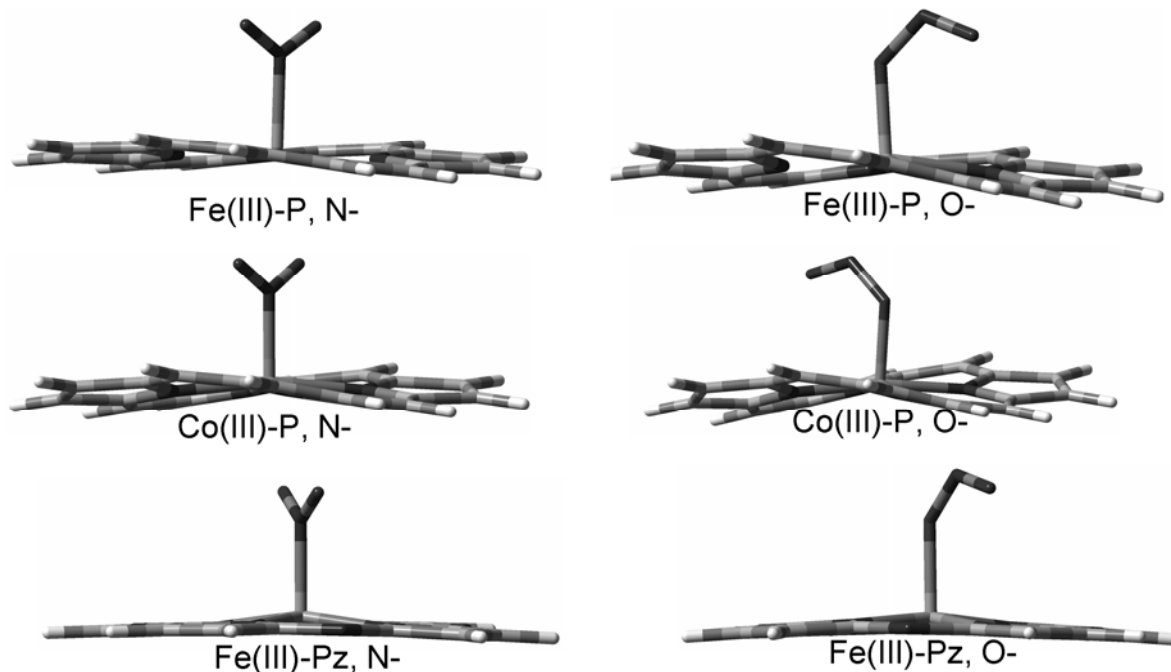


Fig. 2 – Representative geometries for nitro and nitrito models; labeling is as in Tables 2-4.

Table 3

Relevant distances (Å), partial atomic charges and spin densities (the latter shown in brackets) for iron-containing Table 2 models. “m” denotes the macrocycle (P, Pz, Pc, as defined in text and Table 2). “Dt” indicates distortion types in the macrocycle: d=domed, s=saddled

model	Fe-N(m)	Fe-N	N-O ^a	Dt	Fe-O	Fe	N	O ^a	m ^b
S=1/2 Fe(I) P N-	2.00	1.83	1.26	s	2.68	1.03 [0.19]	0.19 [-0.01]	-0.39 [-0.01]	-2.42 [0.83]
S=1/2 Fe(I) P O-	2.00	3.18	1.31/1.25	d	2.13/3.41	0.98 [2.14]	0.14 [0.02]	-0.40/-0.37 [0.11, 0.03]	-2.35 [-1.30]
S=1/2 Fe(I) Pz N-	1.94	1.89	1.25	d	2.72	1.04 [0.38]	0.20 [-0.02]	-0.37 [-0.01]	-2.50 [0.65]
S=1/2 Fe(I) Pz O-	1.93	3.17	1.31/1.25	d	2.14/3.37	0.99 [2.19]	0.16 [0.04]	-0.39/-0.36 [0.12, 0.03]	-2.40 [-1.38]
S=1/2 Fe(I) Pc N-	1.94	1.85	1.25	d	2.69	1.05 [0.26]	0.20 [-0.01]	-0.36 [-0.01]	-2.53 [0.76]
S=1/2 Fe(I) Pc O-	1.93	3.12	1.31/1.24	d	2.12/3.29	0.99 [1.95]	0.17 [0.04]	-0.40/-0.35 [0.12, 0.02]	-2.41 [-1.13]
S=0 Fe(II) P N-	1.98	1.85	1.25	s	2.68	1.06	0.20	-0.36	-1.54
S=0 Fe(II) P O-	1.98	2.91	1.33/1.23	s	1.86/3.18	1.06	0.21	-0.36/-0.31	-1.40
S=0 Fe(II) Pz N-	1.91	1.86	1.25	d	2.69	1.06	0.21	-0.34	-1.59
S=0 Fe(II) Pz O-	1.91	2.89	1.32/1.22	d	1.87/3.14	1.07	0.23	-0.36/-0.29	-1.65
S=0 Fe(II) Pc N-	1.93	1.86	1.25	d	2.69	1.05	0.21	-0.33	-1.60
S=0 Fe(II) Pc O-	1.92	2.91	1.32/1.23	d+s	1.87/3.18	1.07	0.23	-0.35/-0.28	-1.47
S=1/2 Fe(III) P N-	1.98	1.86	1.24	s	2.67	1.15 [1.08]	0.22 [-0.04]	-0.29 [-0.02]	-0.83 [-0.00]
S=1/2 Fe(III) P O-	1.97	2.87	1.34/1.21	s	1.86/3.09	1.15 [1.10]	0.27 [-0.03]	-0.36/-0.24 [-0.04, 0.01]	-0.82 [-0.04]

Table 3 (continued)

S=1/2 Fe(III) Pz N-	1.93	1.90	1.23	d	2.71	1.14 [1.08]	0.24 [- 0.05]	-0.27 [-0.03]	-0.84 [-0.07]
S=1/2 Fe(III) Pz O-	1.92	2.92	1.33/1. 21	d	1.89/3. 13	1.14 [1.18]	0.30 [- 0.07]	-0.34/-0.24 [-0.05, -0.03]	-0.86 [-0.03]
S=1/2 Fe(III) Pc N-	1.94	1.86	1.24	d	2.67	1.15 [1.03]	0.23 [- 0.04]	-0.28 [-0.02]	-0.82 [0.05]
S=1/2 Fe(III) Pc O-	1.95	2.87	1.33/1. 21	d+s	1.86/3. 10	1.15 [1.13]	0.30 [- 0.05]	-0.35/-0.24 [-0.04, 0.02]	-0.86 [-0.00]

^a nitrite oxygens; where values are identical, only one value is listed. ^b sum over all atoms in the macrocyclic ligand.

Spin densities on the macrocycle are generally negligible, with the exception of the iron and cobalt (I) complexes. In these two cases, 0.7 – 1.1 spin units are found delocalized on the macrocycle. Along with the difference in electrical charge, which between M(II) and M(I) complexes is also mostly located on the macrocycle, these data suggest that the electron injected into the system upon formal reduction of the metal (II) adducts to metal (I) resides mostly on the macrocycle, which thus is described as anion radical with the metal retaining its +2 formal oxidation state. On the other hand, the electronic structure at the metal in the low-valent states is remarkably controlled by the nitrite binding mode. This can be seen in spin densities at the metal, which in the iron (I) nitro isomers are close to zero, while in the nitrito isomers they are close to two units. Thus, the formally Fe(I) systems are better described as S=0 Fe(II) + S=1/2 macrocycle anion for the nitro isomers, and S=1 Fe(II) antiferromagnetically coupled to S=1/2 macrocycle anion for the nitrito isomers. This local change in spin state at the iron may be correlated with the distinctly weaker Fe-O bond compared to the Fe-N bond in the “Fe(I)” nitrito vs nitro isomers. This trend, where ‘super-reduced’ metal porphyrinate centers are found to localize the extra electrons on the macrocycle and not on the metal, are in line with our previous observations on formally Fe(0) porphyrinates.¹¹ The cobalt (I) adducts follow the same trend; since these are formally S=0 complexes, one spin unit on

the cobalt is found antiferromagnetically coupled to one spin unit on the macrocycle regardless of nitrite binding mode, and the systems appear well described as Co(II) + macrocycle anion radical.

Scheiner et al have previously examined ‘super-reduced’ Fe(I) and Co(I) phthalocyaninates axially-unsubstituted, optimizing their geometries using symmetry constraints according to by experimental data on metal (II) or metal (III) cognates. The electronic structures in these axially unsubstituted systems were found to be well-described as Fe(I) and Co(I), respectively,^{12,13} with the cobalt case confirming prior assignments based on experiment.¹⁴ By contrast, here and elsewhere¹¹ we have shown that reduction of axially-substituted heme-type macrocycles beyond the metal(II) stage typically entails reduction of the macrocycle rather than at the metal; this is not surprising, since the presence of the axial ligands raises precisely the energies of the d_{z^2} orbitals, where the added electron would reside upon reduction of metal (II). On the other hand, Co(I) centers are generally accepted in biochemistry as part of catalytic cycles in B12 (cobalamin) systems, where axial ligands do exist.¹⁵ We note, however, that the corrin ring found as a ligand to cobalt in cobalamin is much less conjugated than those examined here, and that therefore it is expected that corrin would be less able to delocalize reducing equivalents compared to porphyrin, porphyrazine or phthalocyanine.

Table 4

Relevant distances (Å), partial atomic charges and spin densities (the latter shown in brackets) for cobalt-containing Table 2 models. Labels are as in Table 3

model	Co-N(m)	Co-N	N-O ^a	Dt	Co-O	Co	N	O ^a	m ^b
S=0 Co(I) P N-	1.99	2.05	1.26	s	2.90	0.82 [0.78]	0.17 [0.13]	-0.41 [0.05]	-2.17 [-1.01]
S=0 Co(I) P O-	1.98	3.14	1.30/1. .25	s	2.10/3. .36	0.79 [0.85]	0.15 [0.04]	-0.37/-0.37 [0.12/0.02]	-1.98 [-1.01]
S=0 Co(I) Pz N-	1.92	2.09	1.26	d	2.93	0.81 [0.70]	0.20 [0.15]	-0.39 [0.06]	-2.23 [-0.97]
S=0 Co(I) Pz O-	1.91	3.13	1.30/1. .25	d	2.12/3. .33	0.79 [0.76]	0.16 [0.06]	-0.36 [0.14/0.03]	-2.23 [-0.99]

Table 3 (continued)

S=0 Co(I) Pc N-	1.93	2.06	1.26	d	2.90	0.83 [0.65]	0.19 [0.15]	-0.38 [0.07]	-2.26 [-0.94]
S=0 Co(I) Pc O-	1.93	3.09	1.30/1 .24	d	2.10/3 .26	0.81 [0.70]	0.18 [0.06]	-0.36/-0.34 [0.15/0.03]	-2.30 [-0.94]
S=1/2 Co(II) P N-	1.97	2.06	1.26	s	2.90	0.84 [0.87]	0.19 [0.15]	-0.37 [0.07]	-1.29 [-0.14]
S=1/2 Co(II) P O-	1.97	3.09	1.30/1 .24	d+s	2.09/3 .29	0.83 [0.87]	0.19 [0.06]	-0.36/-0.34 [0.15/0.04]	-1.32 [-0.12]
S=1/2 Co(II) Pz N-	1.90	2.11	1.25	d	2.92	0.83 [0.88]	0.21 [0.17]	-0.35 [0.07]	-1.32 [-0.11]
S=1/2 Co(II) Pz O-	1.90	3.08	1.30/1 .24	d	2.11/3 .25	0.83 [0.95]	0.21 [0.08]	-0.35/-0.33 [0.17/0.05]	-1.36 [-0.25]
S=1/2 Co(II) Pc N-	1.93	2.16	1.24	d+s	2.96	0.84 [0.80]	0.21 [0.14]	-0.34 [0.09]	-1.32 [-0.12]
S=1/2 Co(II) Pc O-	1.91	3.06	1.30/1 .24	d	2.09/3 .23	0.84 [0.87]	0.22 [0.08]	-0.36/-0.32 [0.17/0.05]	-1.40 [-0.17]
S=0 Co(III) P N-	1.97	1.85	1.24	s	2.65	0.95	0.26	-0.29	-0.63
S=0 Co(III) P O-	1.96	2.85	1.31/1 .22	s	1.86/3 .12	0.96	0.28	-0.32/-0.25	-0.67
S=0 Co(III) Pz N-	1.90	1.86	1.23	d	2.65	0.94	0.27	-0.27	-0.70
S=0 Co(III) Pz O-	1.90	2.85	1.30/1 .21	d+s	1.88/3 .13	0.96	0.31	-0.31/-0.24	-0.72
S=0 Co(III) Pc N-	1.93	1.86	1.23	d	2.65	0.95	0.27	-0.27	-0.69
S=0 Co(III) Pc O-	1.92	2.86	1.30/1 .21	d+s	1.87/3 .14	0.95	0.31	-0.31/-0.24	-0.71

^a nitrite oxygens; where values are identical, only one value is listed. ^b sum over all atoms in the macrocyclic ligand.

EXPERIMENTAL

UBP86 and UB3LYP calculations with LANL2DZ and 6-31G** basis sets and were performed within the Gaussian98¹⁶ suite of programs. Solvation calculations employed the SCRF procedure within Gaussian 98,¹⁶ using the UB3LYP/6-31G** functional and the polarized continuum model (PCM)¹⁷ or the Cosmo (CPCM) model¹⁸ with the default solvents number 13 and 1 (dielectric constants 4.335 and 80, respectively).

CONCLUSIONS

Trends have been identified in factors controlling nitrite linkage isomerism in iron porphyrinates and related complexes, which also offer insight into the electronic and geometric structure of an emerging class of 'super-reduced' metal centers. Factors other than those examined here may also be at work in controlling nitro-nitrito isomerism. Thus, in a preliminary study the effect of an axial ligand on the nitro/nitrito preference was gauged by inclusion of an imidazole ligand trans to the nitrite in the Fe(II) and Fe(III) porphyrinate models. It was found that this

addition of an axial ligand had a negligible effect on the Fe(III) models (the 6.9 kcal/mol of Table 2 was increased to 7.6 kcal/mol in the +imidazole model), but it did favor significantly the nitrito isomer in the Fe(II) model (the 10.7 kcal/mol value of Table 2 was decreased to only 1.1 kcal/mol in the +imidazole model). Further work is under way to systematically examine the ways in which axial ligation may be used to tune linkage isomerism and reactivity in metal-nitrite complexes.

Acknowledgements: Funding from a joint Russian Foundation for Basic Research/Roumanian Academy (to SVM and RSD), as well as from the Roumanian government (PNII-Ideas project 565/2007 and CEEEx-ET 48/2006) is gratefully acknowledged.

REFERENCES

1. R. Silaghi-Dumitrescu, *Inorg. Chem.*, **2004**, *43*, 3715-3718.
2. E.V. Kudrik, S.V. Makarov, A. Zahl, R. van Eldik, *Inorg Chem.*, **2003**, *42*, 618-24.
3. E.V. Kudrik, S.V. Makarov, A. Zahl, R. van Eldik, *Inorg Chem.*, **2005**, *44*, 6470-5.
4. R. Silaghi-Dumitrescu, *J Inorg Biochem.*, **2006**, *100*, 396-402.
5. D.M. Copeland, A.S. Soares, A.H. West, G.B. Richter-Addo, *J Inorg Biochem.*, **2006**, *100*, 1413-25.

6. J. Yi, M.K. Safo, G.B. Richter-Addo, *Biochemistry*, **2008**, *47*, 8247-9.
7. M.T. Gladwin, R. Grubina, M.P. Doyle, *Acc Chem Res*, **2009**, *42*, 157-67.
8. M.T. Gladwin, *Nat Chem Biol*, **2005**, *1*, 245-6.
9. R. Silaghi-Dumitrescu, I. Silaghi-Dumitrescu, *J Inorg Biochem*, **2006**, *100*, 161-6.
10. J.A. Shelnut, X.-Z. Song, J.-G. Ma, S.-L. Jia, W. Jentzen, C.J. Medforth, *Chem. Soc. Rev.*, **1998**, *27*, 31-41.
11. Z. Kis, R. Silaghi-Dumitrescu, *Int. J. Quant. Chem.*, **2009**, *in press*.
12. M.-S. Liao, S. Scheiner, *J Comput Chem*, **2002**, *23*, 1391-1403.
13. M.-S. Liao, S. Scheiner, *J. Chem. Phys.*, **2001**, *114*, 9780-9791.
14. L.D. Rollman, T. Iwamoto, *J Am Chem Soc*, **1968**, *90*, 1455-1463.
15. L.D. Slep, F. Neese, *Angew. Chem. Int. Ed.*, **2003**, *42*, 2942-2945.
16. Gaussian 98 (Revision A.1), M. J. Frisch, G. W. Trucks, H. B. Schlegel, G. E. Scuseria, M. A. Robb, J. R. Cheeseman, V. G. Zakrzewski, J. A. Montgomery, R. E. Stratmann, J. C. Burant, S. Dapprich, J. M. Millam, A. D. Daniels, K. N. Kudin, M. C. Strain, O. Farkas, J. Tomasi, V. Barone, M. Cossi, R. Cammi, B. Mennucci, C. Pomelli, C. Adamo, S. Clifford, J. Ochterski, G. A. Petersson, P. Y. Ayala, Q. Cui, K. Morokuma, D. K. Malick, A. D. Rabuck, K. Raghavachari, J. B. Foresman, J. Cioslowski, J. V. Ortiz, B. B. Stefanov, G. Liu, A. Liashenko, P. Piskorz, I. Komaromi, R. Gomperts, R. L. Martin, D. J. Fox, T. Keith, M. A. Al-Laham, C. Y. Peng, A. Nanayakkara, C. Gonzalez, M. Challacombe, P. M. W. Gill, B. G. Johnson, W. Chen, M. W. Wong, J. L. Andres, M. Head-Gordon, E. S. Replogle and J. A. Pople, Gaussian, Inc., Pittsburgh PA, 1998.
17. S. Miertus, E. Scrocco, J. Tomasi, *Chem.Phys.*, **1981**, *55*, 1645-1652.
18. V. Barone, M. Cossi, *J. Phys Chem. A*, **1998**, *102*, 1995.